Evaluation of crack-terminating angles in heat-treated silica DCDC-specimens
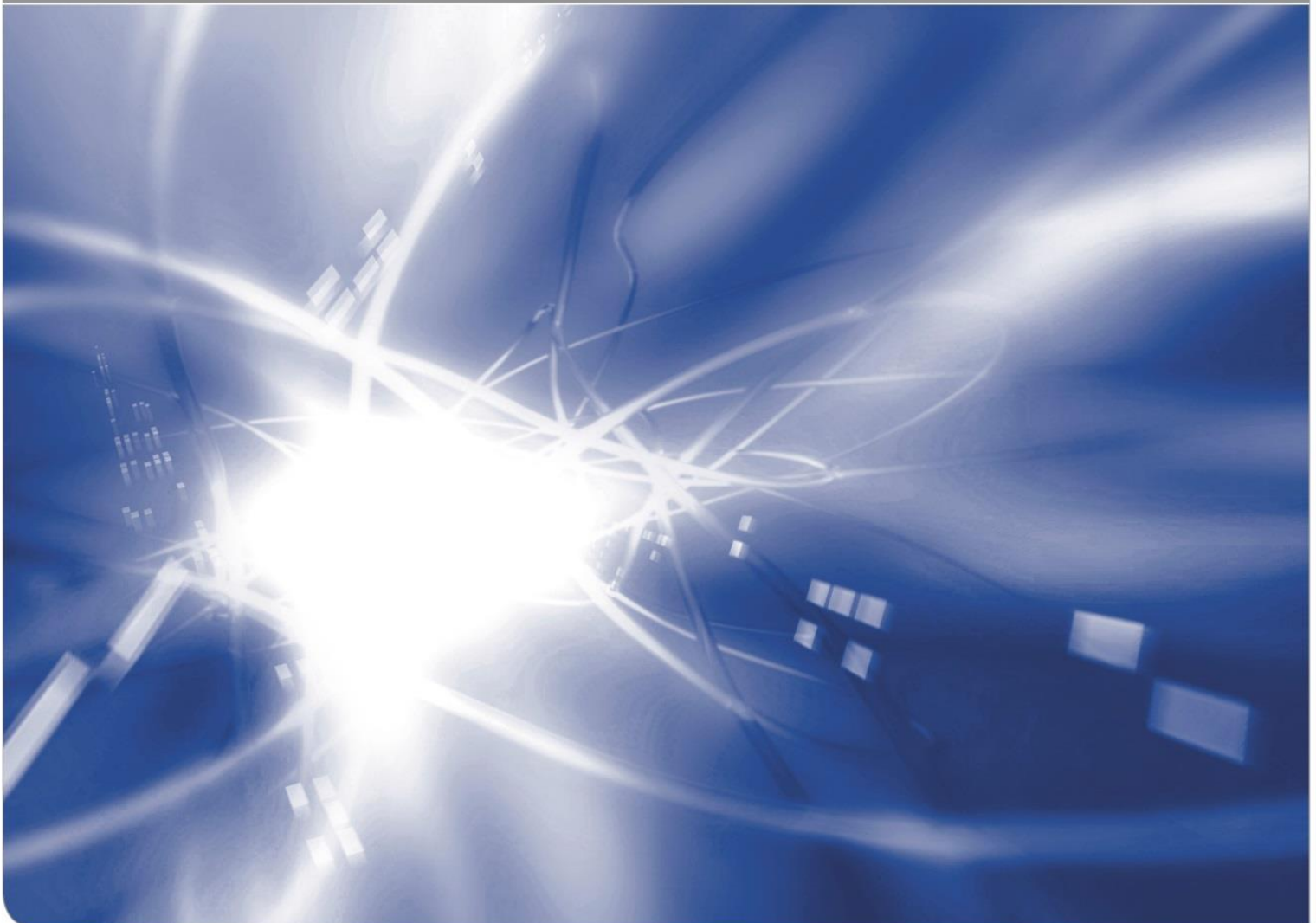
P. Hettich, K. G. Schell, G. Rizzi, S. Wagner, T. Fett

Karlsruhe Institute of Technology (KIT)

Institute for Applied Materials – Ceramic Materials and Technologies

Abstract

Cracks terminating at free surfaces are affected by local stresses in the surface region. Under residual compression, the crack front must retard and under residual tensile stresses advance, both compared with the crack contour in the absence of stresses. This effect can be used for an estimation of residual surface stresses in silica generated during the silica/water reaction and caused by volume swelling. A strong shielding stress intensity factor of about -2.5 MPa√m was found for DCDC specimen heat-treated for 192h at 250°C in water. This result is a clear indication for compressive stresses developing in the water diffusion zone at the surface.

Contents

1. Introduction

In an earlier paper [1] we described a method for the identification of stresses in the surface region by the observation of crack-terminating angles of Vickers indentation cracks. The procedure was applied to chemically strengthened soda-lime glass [2] and to surface layers after water soaking undergoing ion exchange [3,4].

When water comes in contact with silica [SiO_2], it reacts with the silica network according to

$$\equiv\text{Si-O-Si}\equiv +H_2O \leftrightarrow \equiv\text{SiOH}+\text{HOSi}\equiv \tag{1}$$

where [$\equiv$SiOH]=S is the hydroxyl and [H_2O]=C is the concentration of the molecular water. This reaction results in a volume swelling [5,6,7,8] and, since the free expansion in the thin layer is restricted, in negative swelling stresses [9]. Such stresses at a free specimen surface must affect the crack front contours of cracks ending at these surfaces. The present paper deals with the determination of the terminating angles.

Figure 1 shows a crack growing from left to right in a bar with residual stresses in thin surface layers. The crack front terminates at the free surface under an angle φ.

If compressive stresses (expansive strains) occur at the surfaces, the actual crack front in a crack growth test under superimposed external load must stay behind (Fig. 1a). In contrast, tensile stresses caused by shrinking effects must result in an advance of the crack (Fig. 1b).
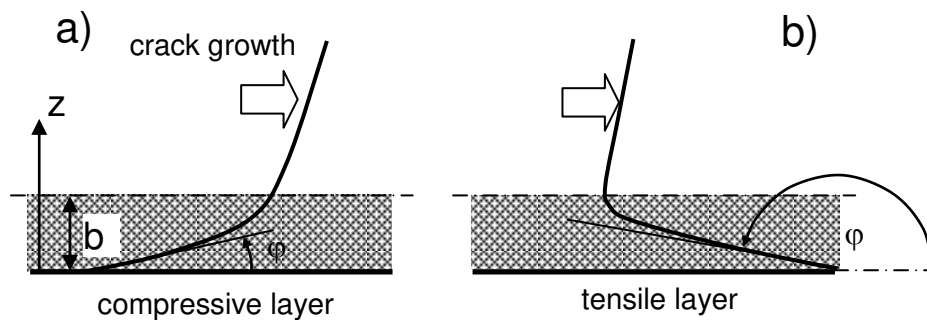

Fig. 1 Crack fronts terminating at the specimen surface under an angle φ, a) crack retard in a zone of compressive stresses, b) crack advance by tensile stresses. Arrows indicate crack growth direction.

2. Stress intensity factor solutions

The problem of a crack-front intersecting a free surface has often been studied in theoretical fracture mechanics and was also discussed in [1]. From curves reported in [10] it can be concluded that the ½-singularity of stresses characterizing the stress intensity factor is only possible for a crack terminating angle of

$$\varphi \cong 90° - 38.8°\,\nu \tag{2}$$

For most brittle materials with ν≈0.25, the crack terminating angle is about φ≈80°, i.e. a deviation of 10° from the normal. For silica with ν=0.17 we have to expect: φ≅83°.

Stress intensity factors for DCDC-specimens were determined by 3-dimensional FE computations on materials with Poisson ratios in the range of $0<\nu\leq0.25$. In [1] the results were reported for $\nu=0.25$ as fits to soda-lime glass. Similar results for the special case of silica with $\nu=0.17$ are represented in Fig. 2a for crack-terminating angles of $\varphi=45°$, $60°$, $83.4°$ and $90°$ in form of the fracture mechanics geometric function F, defined for the DCDC-specimen by

$$F = \frac{K}{|p|\sqrt{\pi R}} \tag{3}$$

In (3) p is the pressure at the end surfaces and R is the radius of the drill hole. The FE-results are introduced as the circles.

We computed stress intensity factors along the crack front for different terminating angles. For estimations on a wide range of terminating angles two theoretical limit cases were included. For $\varphi=0$ it must hold $K(\varphi)\rightarrow\infty$ and for $\varphi=180°$: $K(\varphi)=0$ (see e.g. Fenner and Abdul Mihsein [11]). The stress intensity factors as a function of the terminating angle are given in a normalized representation in Fig. 2b recommended for interpolations in the region $\varphi\leq90°$.

In order to allow similar computations, an approximate equation for $\nu=0.17$ may be applied

$$\frac{K(\varphi)}{K(83.4°)} \cong \frac{1}{0.00817\,\varphi+9.5\times10^{-13}\,\varphi^6} \qquad (\varphi \text{ in degree}) \tag{4}$$

that is introduced in Fig. 2b as the interpolation curve.

When residual stresses are present at the surfaces at which a crack terminates, they affect the crack tip stress field by generating an additional stress intensity factor. Since for compressive stresses the crack tip is partially shielded from the externally applied stresses, it may be called "shielding" stress intensity factor, K_{sh}.

Following the superposition priciple of linear-elastic fracture mechanics, the total stress intensity factor K_{tip} is the superposition of the applied one, K_{appl}, and the shielding stress intensity factor, K_{sh}. Under stable crack growth conditions, the total stress intensity factor as the sum must equal the fracture toughness K_{Ic}:

$$K_{tip} = K_{appl} + K_{sh} = K_{Ic} \tag{5}$$

Then the terminating angle at an un-toughened surface must fulfil $K_{tip}=K_{Ic}$. The fracture toughness of silica is at room temperature $K_{Ic} \cong 0.8$ MPa√m as reported by Wiederhorn [12].In the absence of a side surface layer by water soaking, $K_{sh}=0$, it − follows from eq.(5) simply that $K_{tip}=K_{appl}$. Under conditions of subcritical crack growth we measured crack-growth rates of about 10^{-4}m/s. In this case, it follows from measurements by Wiederhorn and Bolz [13] that the stress intensity factor is $\cong0.57$ MPa√m. Since in these tests the terminating angle is in good agreement with the prediction of $\varphi=84.3°$ as is predicted via eq.(2). Consequently, the experimentally

obtained value of $K_{\text{appl}}(83.4°) = 0.57$ MPa√m has to be introduced on the right-hand side of eq.(5). Then it results

$$\frac{K(\varphi)}{K_{Ic}} = \frac{K_{appl}}{K_{Ic}} = \frac{K(\varphi)}{K(\varphi_0)} \tag{6}$$
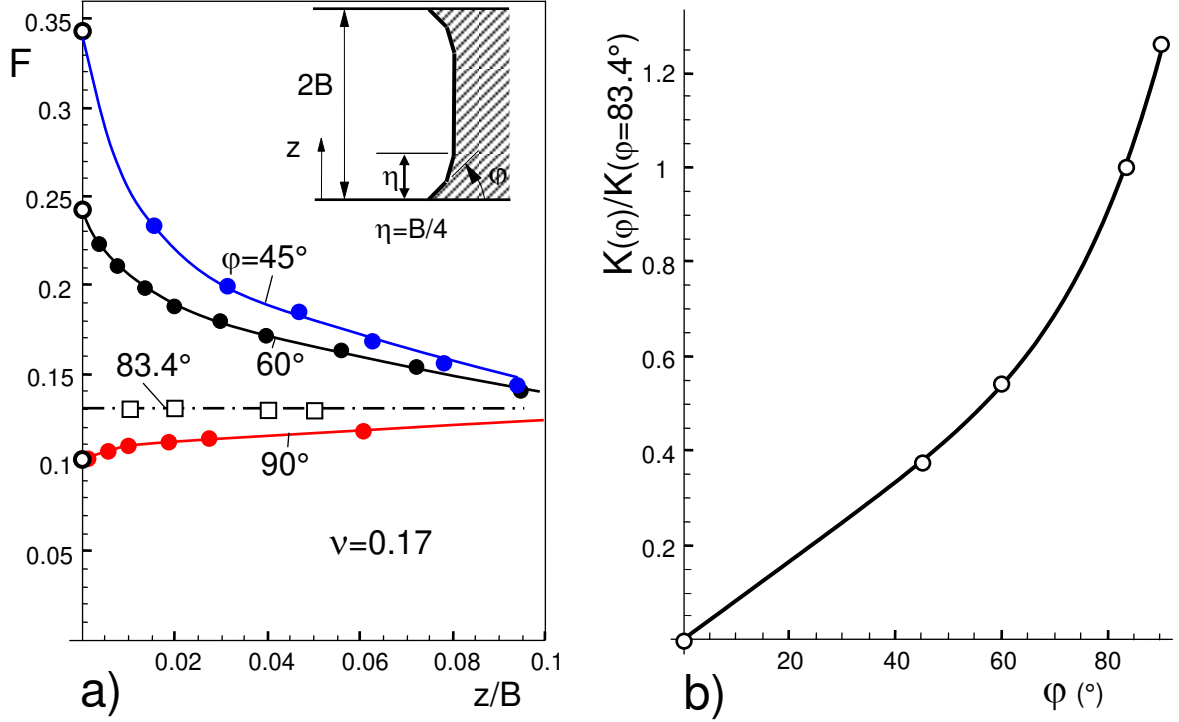

Fig. 2 a) Stress intensity factors at the surface region of cracks terminating under different angles φ in terms of the geometric function *F* according to eq.(3), b) surface stress intensity factor normalized on the value for φ=83.4°, curve: interpolation following equation (4).

Volume expansions occur by swelling of the glass volume due to hydroxyl generation [9, 14, 15]. Such a swelling effect in water-containing silica at high temperatures was early reported by Brückner [5,6], Shackelford [7] and Shelby [8].

These authors showed that the density decreased by reaction eq.(1) at high temperatures is

$$\frac{\Delta\rho}{\rho_0} = -\chi\, C_w \tag{7}$$

where C_w is the weight fraction of water. From the definition of the density as the quotient of mass *m* and volume *V*, ρ=*m*/*V*, it follows for an increased water concentration Δ*m* a volume swelling strain ε_v

$$\varepsilon_v = \frac{\Delta V}{V} = \frac{\Delta m}{m} - \frac{\Delta\rho}{\rho} \tag{8}$$

The result for ε_v can be expressed after [5-8] by

$$\varepsilon_v = 1.84\, C_w = \kappa\, S \;, \quad \kappa = 0.97\,[0.92,1.02] \tag{9}$$

3

By mechanical boundary conditions, the swelling strains result in swelling stresses proportional to the amount of hydroxyl concentration. The effect of the water-silica reaction is the generation of *swelling strains*. *Swelling stresses* are a consequence of the mechanical boundary conditions. A volume element in a thick plate that undergoes swelling cannot freely expand. If the diffusion zone is small compared to the component dimensions, expansion is completely prevented in the plane of the surface and can only take place normal to the surface plane. In the absence of externally applied stresses no preference in swelling strains is given and therefore *isotropic swelling* in all directions has to be expected.

At a free surface, the stress state is plane stress and, consequently, also stresses caused by swelling are equi-biaxial ($\sigma_{sw,z}=0$)

$$\sigma_{sw,y} = \sigma_{sw,x} = -\frac{\varepsilon_v E}{3(1-\nu)} = -\frac{\kappa E}{3(1-\nu)} S \qquad (10)$$

where E is Young's modulus and ν is Poisson's ratio and $\kappa=0.97$ [9]. The depth distribution in the diffusion zone is then

$$\sigma_{sw} = \sigma_{sw,0} \, \mathrm{erfc}\left[\frac{y}{2b}\right] \qquad (11)$$

The occurrence of compressive stresses can now be proved by the observation of crack terminating angles and computation of the crack-shielding stress intensity factors that are proportional to the swelling stresses

$$K_{sh} \propto \sigma_{sw,y} \sqrt{b} \qquad (12)$$

The diffusion distance b, an appropriate measure for the thickness of the diffusion zone (where the water concentration is roughly half of that at the surface) is given by

$$b = \sqrt{D_w t} \qquad (13)$$

(t=time). Water diffusion into the surface of silica glass has been studied experimentally by a number of investigators, and shown to depend on temperature according to

$$D_w = A_0 \exp[-Q_w / RT] \qquad (14)$$

Q_w is the activation energy, T is the absolute temperature, and R is the gas constant. As reported by Zouine et al. [16] for silica in the temperature range 0 °C to 200 °C: Q_w = 72.3 kJ/mol, $\log_{10} A_0$ = -8.12 (A_0 is in m^2/s).

3. Measurements and evaluation

We studied crack terminating angles on DCDC-specimens [17] of the silica glass EN08NB (GVB, Herzogenrath, Germany) containing 99.98% SiO_2. DCDC-specimens were prepared and annealed at 1150°C for 1h in vacuum in order to remove residual stresses from machining. Then the specimens were heat-treated in water at 250°C for

192h and 48h. Afterwards, fast DCDC-tests under increasing load were performed with partial unloading for the generation of crack-arrest markings on the fracture surface. Final fracture was obtained by introducing a needle with an excessive diameter into the DCDC-hole.

Figure 3a shows the result for a specimen without heat treatment. The terminating angle of 83° expected from eq.(3) is tentatively introduced by the straight lines showing sufficient agreement with the crack contours.

A specimen after 192h at 250°C water vapour treatment is shown in Fig. 3b. This image shows clearly deviating terminating angles of only $\varphi \cong 25°$ as is indicated by the straight line. A specimen after a 192h, 250°C liquid-water soaking is given in Fig. 3c. In this case, the terminating angles are about $\varphi \cong 30°$. The size of the diffusion zone b is introduced by the arrows.

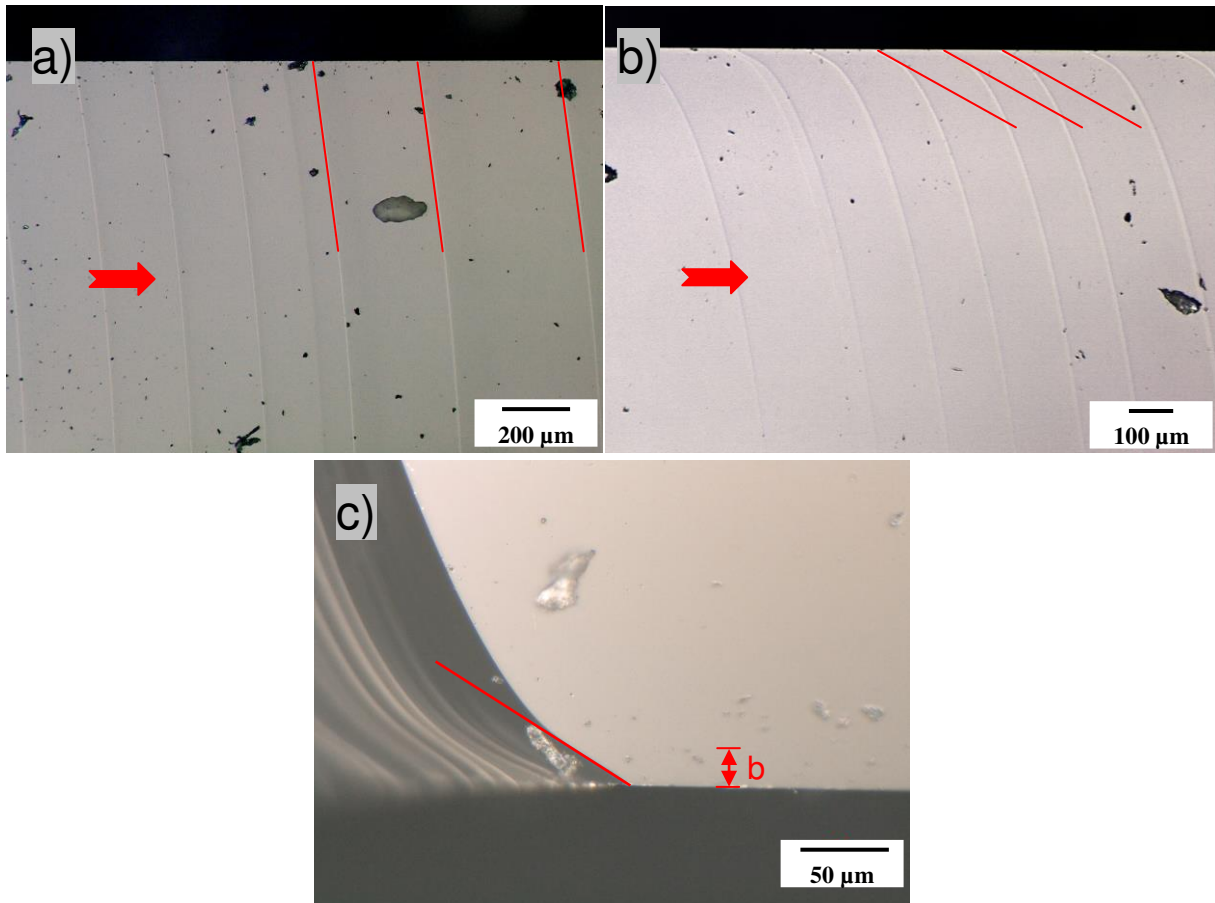**Fig. 3** Crack terminating angles in DCDC-specimens, a) without hot-water soaking (theoretical angles of $\varphi \cong 83°$ tentatively introduced as the tangents, b) after 192h 250°C soaking in water vapour at saturation pressure, c) after 192h 250°C soaking in liquid water.

Figure 4 shows typical crack arrest contours on the fracture surface for a specimen liquid-water heat-treated for 48h at 250°C. The terminating angles for this condition are about $\varphi \cong 41°$.

Finally, Table 1 compiles the relevant test data and the experimental findings. The crack terminating angles are listed in column 3 as the average angle and the standard deviation, SD. The layer thicknesses for the liquid-water soaked specimens are com-

piled in column 4. The layers for the water-soaked specimens may be slightly smaller, because some dissolution of silica in water cannot be excluded. The approximation signs indicate this. Column 5 shows the applied stress intensity factors, K_{appl}, normalized on the value $K_{appl,0}$ for specimens without heat treatment as resulting from eq.(4). Column 6 gives the stress intensity factors for the crack extension under subcritical and spontaneous crack growth conditions. In the case of liquid water tests for the 250°C/192h-condition, we evaluated the first crack contour as is visible after spontaneous crack propagation starting from the hole. The applied stress intensity factors are given in column 7. Strongly negative shielding stress intensity factors $K_{sh}<0$ are observed in all cases, indicating strong compressive stresses in the water diffusion layer, column 8.
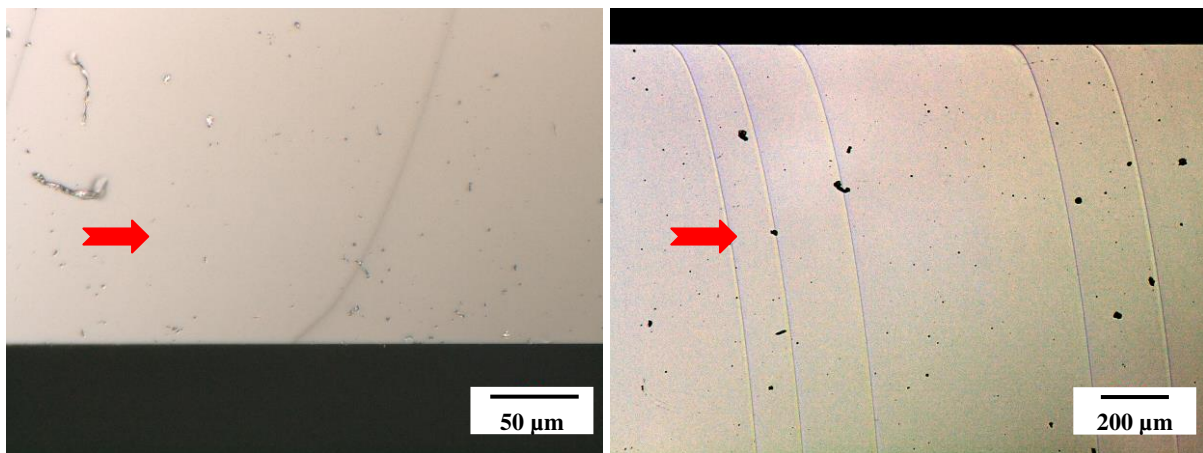

Fig. 4 Typical crack fronts for a specimen with 48h/250°C heat treatment.

Water	t (h)	Terminating angle φ	b, eq.(11) (µm)	$K_{appl}/K_{appl,0}$	$K_{appl,0}$ (MPa√m)	K_{appl} (MPa√m)	K_{sh} (MPa√m)
–	0	83.4°	0	1	0.57	0.57	0
vapour	192	25° (SD=1.2°)	17.7	4.90	0.57	2.94	−2.37
liquid	48	41.0° (SD=1.36°)	≈8.9	2.95	0.57	1.77	−1.20
liquid	192	29.8° (29.3/30.3)	≈17.7	4.3	0.8	3.44	−2.64

Table 1 Experimental results; $K_{appl,0}$ is the applied stress intensity factor in specimen without heat treatment.

Summary:

The silica/water reaction at silica surfaces exposed to water causes volume expansion in the water diffusion layer and as the consequence of mechanical boundary conditions compressive stresses. For the estimation of the shielding stress intensity factor for cracks passing this layer, we applied a method developed in [1] that was demonstrated on Vickers indentation cracks in soda-lime glass. Evaluation of crack-terminating angles resulted in strongly negative shielding stress intensity factors of about −2.5 MPa√m, a clear evidence for compressive stresses in the water-affected surface layer.

References

1 K.G. Schell, S. Wagner, P. Hettich, T. Fett, G. Rizzi, M.J. Hoffmann, Identification of residual stress layers at glass surfaces via crack terminating angles, J. Am. Ceram. Soc. **100** (2017), 4173-4179.

2 T. Haranoh, H. Ishikawa, N. Shinkai, M. Mizuhashi, Crack evolution in Vickers indentation for soda-lime-silica glass, J. of Mater. Science **17** (1982) 1493-1500.

3 W.A. Lanford, K. Davis, P. Lamarche, T. Laursen, R. Groleau, and R.H.Doremus, "Hydration of Soda-Lime Glass," *J. Non-Cryst. Sol.* **33**, 249-266 (1979).

4 T. Fett, J.P. Guin, and S. M. Wiederhorn, Stresses in ion-exchange layers of soda-lime-silicate glass, Fatigue Fract. Engng. Mater. Struct. **28** (2005), 507-514.

5 Brückner, R., "The structure-modifying influence of the hydroxyl content of vitreous silicas," Glastech. Ber. **43** (1970), 8-12.

6 Brückner, R., "Metastable equilibrium density of hydroxyl-free synthetic vitreous silica," J. Non-Cryst. Solids, **5** (1971), 281-5

7 Shackelford, J.F., Masaryk, J.S., Fulrath, R.M., "Water Content, Fictive Temperature and Density Relations for Fused Silica," J. Am. Ceram. Soc. **53** (1970), 417.

8 Shelby, J.E., "Density of vitreous silica," J. Non-Cryst. **349** (2004), 331-336

9 S. M. Wiederhorn, F. Yi, D. LaVan, T. Fett, M.J. Hoffmann, Volume Expansion caused by Water Penetration into Silica Glass, J. Am. Ceram. Soc. **98** (2015), 78-87.

10 Dimitrov, A., Eckensingularitäten bei räumlichen Problemen der Elastizitätstheorie: Numerische Berechnung und Anwendungen, PhD-Thesis, University of Karlsruhe, 2002.

11 Fenner, D.M., Abdul Mihsein, M.J., Crack front elastic stress state for three-dimensional crack problems, International Journal of Fracture **25** (1984) 121-131.

12 S.M. Wiederhorn, "Fracture Surface Energy of Glass," *J. Am. Ceram. Soc.* **52** [2] 99-105 (1969).

13 S.M. Wiederhorn and L.H. Bolz, Stress Corrosion and Static Fatigue of Glass, J. Am. Ceram. Soc. **53**(1970) 543-548.

14 S.M. Wiederhorn, T. Fett, G. Rizzi, S. Fünfschilling, M.J. Hoffmann and J.-P. Guin, "Effect of Water Penetration on the Strength and Toughness of Silica Glass," *J. Am. Ceram. Soc.* **94** (2011) [S1] S196-S203.

15 T. Fett, G. Rizzi, M. Hoffmann, S. Wagner, and S.M. Wiederhorn, "Effect of Water on the inert Strength of Silica Glass: Role of Water Penetration," *J. Am. Ceram. Soc.* **95** (2012) [12], 3847-3853.

16 Zouine, A., Dersch, O., Walter, G., Rauch, F., Diffusivity and solubility of water in silica glass in the temperature range 23-200°C, Phys. Chem. Glasses, **48** (2007), 85-91.

17 Janssen, C., Specimen for fracture mechanics studies on glass, in Proceedings Xth International Congress on Glass, (1974), p. 23, Kyoto, Japan.